Simulation Of Medical Treatment For Infections After Knee Replacement Surgery

Josh Thomas[1], Luke Gritter[1], Kyle Koppenhoefer[1], Bibin Prasad[2], John Tepper[2], Rajiv Chopra[2]

[1]AltaSim Technologies, Worthington, OH, United States
[2]Solenic Medical, Addison, TX, United States

Abstract

While prosthetic joints can improve people's quality of life, there is an unmet need for the treatment of post-surgery infections. A novel technology has been developed that can treat these infections with electromagnetic heating. A series of anatomical models of knees with implants have been developed for simulation of the heat treatment process. These simulations are supporting the ongoing FDA approval process necessary to make the treatment device commercially available to doctors. Initial CAD of a non-surgically repaired knee was used as a baseline for developing a series of CAD models of surgically replaced knees for analysis. Distinct regions in original knee CAD include skin, bone, muscles, ligaments, tendons, bursa, nerves, veins, and arteries. In consultation with surgeons, appropriate femoral and tibial bone cuts, bone drills, and tissue dissections were performed. Commercially available knee implant system CAD was then indexed and placed in the knee with space left for cement. The final, surgically replaced knee geometry was imported into a COMSOL Multiphysics electromagnetic heating simulation model file of the prototype treatment coil. Extensive troubleshooting and tweaking of the geometry finalization operations and meshing was required for a successful mesh of the complicated assembly of tissues and implant domains. Without a CAD representation of the cement paste applied at the time of surgery, cemented digital versions of the knee implant system were generated using custom partial differential equation (PDE) interfaces in COMSOL to solve for the spatial location of cement as a pre-processing step. Transient thermal simulations for heat-up and cool-down cycles of the coil in operation predict spatial distributions of temperature in the digital knees. Uniform high temperatures (75-80°C) in known regions around the metal and cement are desirable as these are regions where infection is common. On the other hand, damage to healthy tissue is a safety concern. To quantify the effect of desirable and undesirable heating, CEM43 damage integration equations are solved within COMSOL based on the transient temperature field. Numerical results are validated against cadaver studies of the treatment without perfusion effects.

Reference

[1] B. Prasad et al., “Quantifying the relationship between biofilm reduction and thermal tissue damage on metal implants exposed to alternating magnetic fields,” Int. J. Hyperthermia, vol. 39, no. 1, pp. 713–724, 2022, doi: 10.1080/02656736.2022.2065038.
[2] B. Prasad et al., “Role of simulations in the treatment planning of radiofrequency hyperthermia therapy in clinics,” J. Oncol., vol. 2019, 2019, doi: 10.1155/2019/9685476.
[3] B. Prasad et al., “Effect of tumor properties on energy absorption, temperature mapping, and thermal dose in 13.56-MHz radiofrequency hyperthermia,” J. Therm. Biol., vol. 74, no. January, pp. 281–289, 2018, doi: 10.1016/j.jtherbio.2018.04.007.
[4] B. Prasad et al., “Quantitative Estimation of the Equivalent Radiation Dose Escalation using Radiofrequency Hyperthermia in Mouse Xenograft Models of Human Lung Cancer,” Sci. Rep.,

vol. 9, no. 1, p. 3942, 2019, doi: 10.1038/s41598-019-40595-6.
[5] C. H. Hor et al., “Temperature rise by viscous dissipation effect on synovial fluid induced by oscillating motion in artificial hip joint,” Case Stud. Therm. Eng., vol. 24, Apr. 2021, doi: 10.1016/j.csite.2021.100845.
[6] M. N. Moghadam et al., “Impact of synovial fluid flow on temperature regulation in knee cartilage,” J. Biomech., vol. 48, no. 2, pp. 370–374, Jan. 2015, doi: 10.1016/j.jbiomech.2014.11.008.
[7] E. Topsakal et al., “Glucose-dependent dielectric properties of blood plasma,” in 2011 30th URSI General Assembly and Scientific Symposium, URSIGASS 2011, 2011. doi: 10.1109/URSIGASS.2011.6051324.
[8] K. Kurata et al., “Assessment of thermal damage in total knee arthroplasty using an osteocyte injury model,” J. Orthop. Res., vol. 35, no. 12, pp. 2799–2807, 2017, doi: 10.1002/jor.23600.
[9] H. Fukushima et al., “Conduction analysis of cement interface temperature in total knee arthroplasty,” Kobe J. Med. Sci., vol. 48, no. 1–2, pp. 63–72, 2002.
[10] S. Mazzullo et al., “Numerical simulation of thermal bone necrosis during cementation of femoral prostheses*,” 1991.
[11] H. Abu Hassan Shaari et al., “Synthesis and conductivity studies of poly(Methyl methacrylate) (pmma) by co-polymerization and blending with polyaniline (pani),” Polymers, vol. 13, no. 12, Jun. 2021, doi: 10.3390/polym13121939.
[12] U. Abaci et al., “Plasticizer effect on dielectric properties of poly(methyl methacrylate)/titanium dioxide composites,” Polym. Polym. Compos., vol. 29, no. 9_suppl, pp. S565–S574, Nov. 2021, doi: 10.1177/09673911211014757.
[13] L. Melk and N. Emami, “Mechanical and thermal performances of UHMWPE blended vitamin E reinforced carbon nanoparticle composites,” Compos. Part B Eng., vol. 146, pp. 20–27, Aug. 2018, doi: 10.1016/j.compositesb.2018.03.034.
[14] K. S. Cheng et al., “The performance of a reduced-order adaptive controller when used in multi-antenna hyperthermia treatments with nonlinear temperature-dependent perfusion,” Phys. Med. Biol., vol. 54, no. 7, pp. 1979–1995, 2009, doi: 10.1088/0031-9155/54/7/008.
[15] J. A. Groen, et al., “Quantification of tissue property and perfusion uncertainties in hyperthermia treatment planning: Multianalysis using polynomial chaos expansion,” Comput. Methods Programs Biomed., vol. 240, Oct. 2023, doi: 10.1016/j.cmpb.2023.107675.
[16] G. C. Van Rhoon et al., “CEM43°C thermal dose thresholds: A potential guide for magnetic resonance radiofrequency exposure levels?,” Eur. Radiol., vol. 23, no. 8, pp. 2215–2227, 2013, doi: 10.1007/s00330-013-2825-y.
[17] D. M. Yarmolenko et al., “Thresholds for thermal damage to normal tissues : An update,” Int. J. HyperthermiaJournal, vol. 27, no. 4, pp. 320–343, 2011, doi: 10.3109/02656736.2010.534527.Thresholds.
[18] F. Adibzadeh, et al., “SAR thresholds for electromagnetic exposure using functional thermal dose limits,” Int. J. Hyperthermia, vol. 34, no. 8, pp. 1248–1254, 2018, doi: 10.1080/02656736.2018.1424945.
[19] J. Nadobny, et al., “Experimental investigation and histopathological identification of acute thermal damage in skeletal porcine muscle in relation to whole-body SAR, maximum temperature, and CEM43 °c due to RF irradiation in an MR body coil of birdcage type at 123 MHz,” Int. J. Hyperthermia, vol. 31, no. 4, pp. 409–420, Jun. 2015, doi: 10.3109/02656736.2015.1007537.
[20] L. J. Boucher, et al., “RESEARCH AND EDUCATION SECTION EDITOR Temperature threshold levels for heat-induced bone tissue injury: A vital-microscopic study in the rabbit.”
[21] S. S. Chen et al., “Heat-Induced Changes in the Mechanics of a Collagenous Tissue: Isothermal Free Shrinkage,” 1997. [Online]. Available: http://biomechanical.asmedigitalcollection.asme.org/
[22] V. Sadaphal et al., “Feasibility of heating metal implants with alternating magnetic fields (AMF) in scaled up models,” Int. J. Hyperthermia, vol. 39, no. 1, pp. 81–96, 2022, doi:

10.1080/02656736.2021.2011434.

Figures used in the abstract

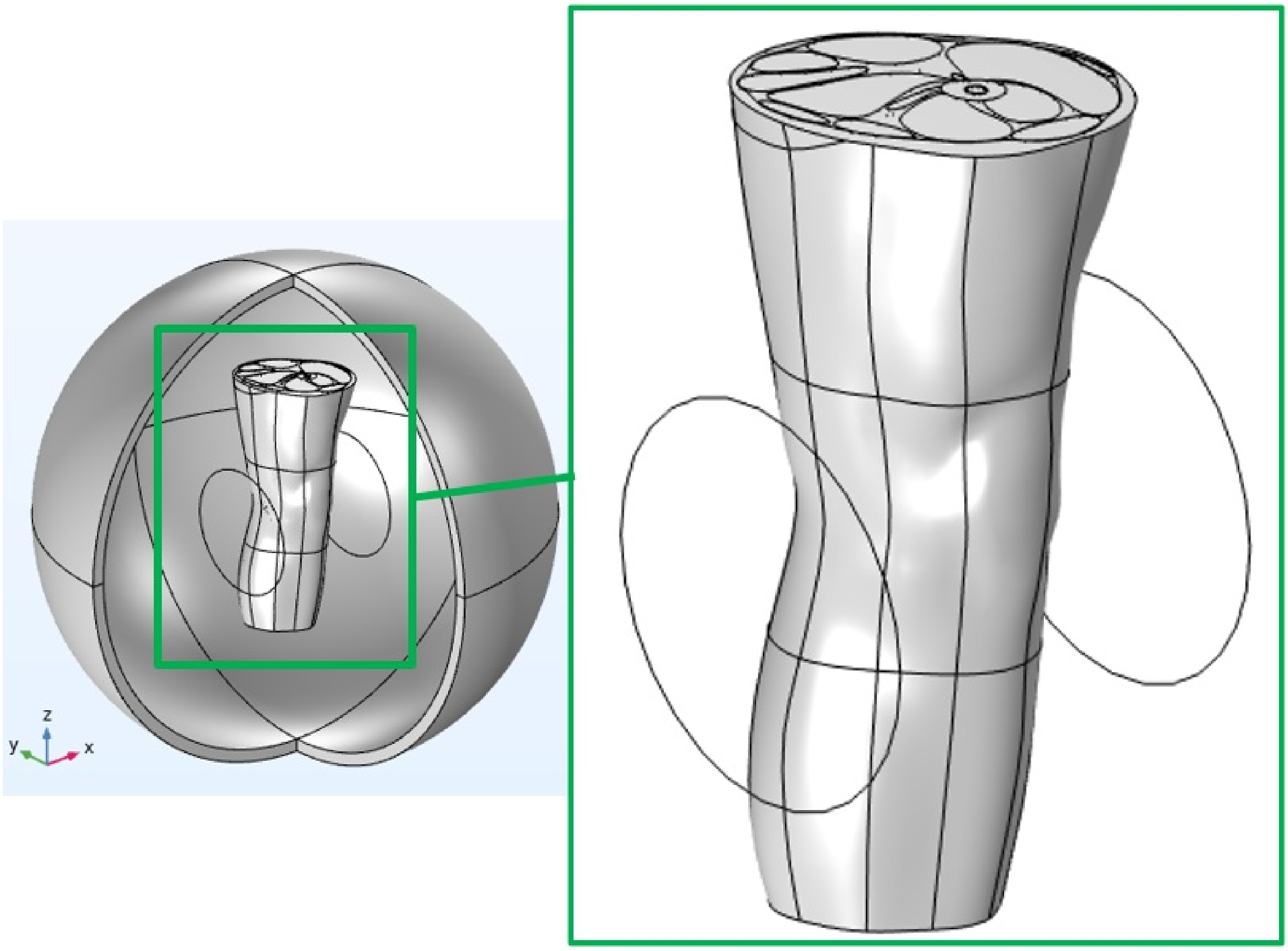

Figure 1 : Computational regions

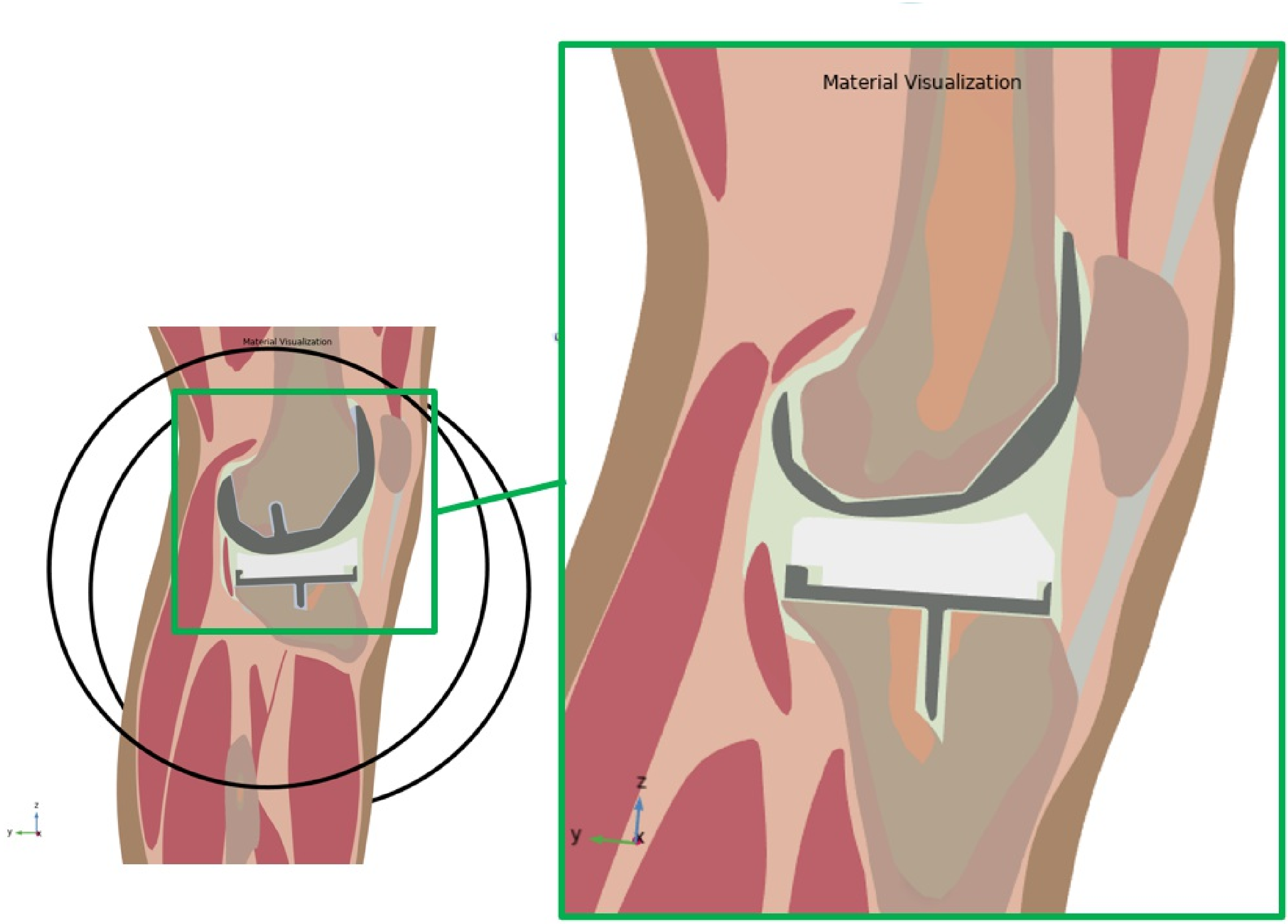

Figure 2 : Slice view of computational regions with material regions colored

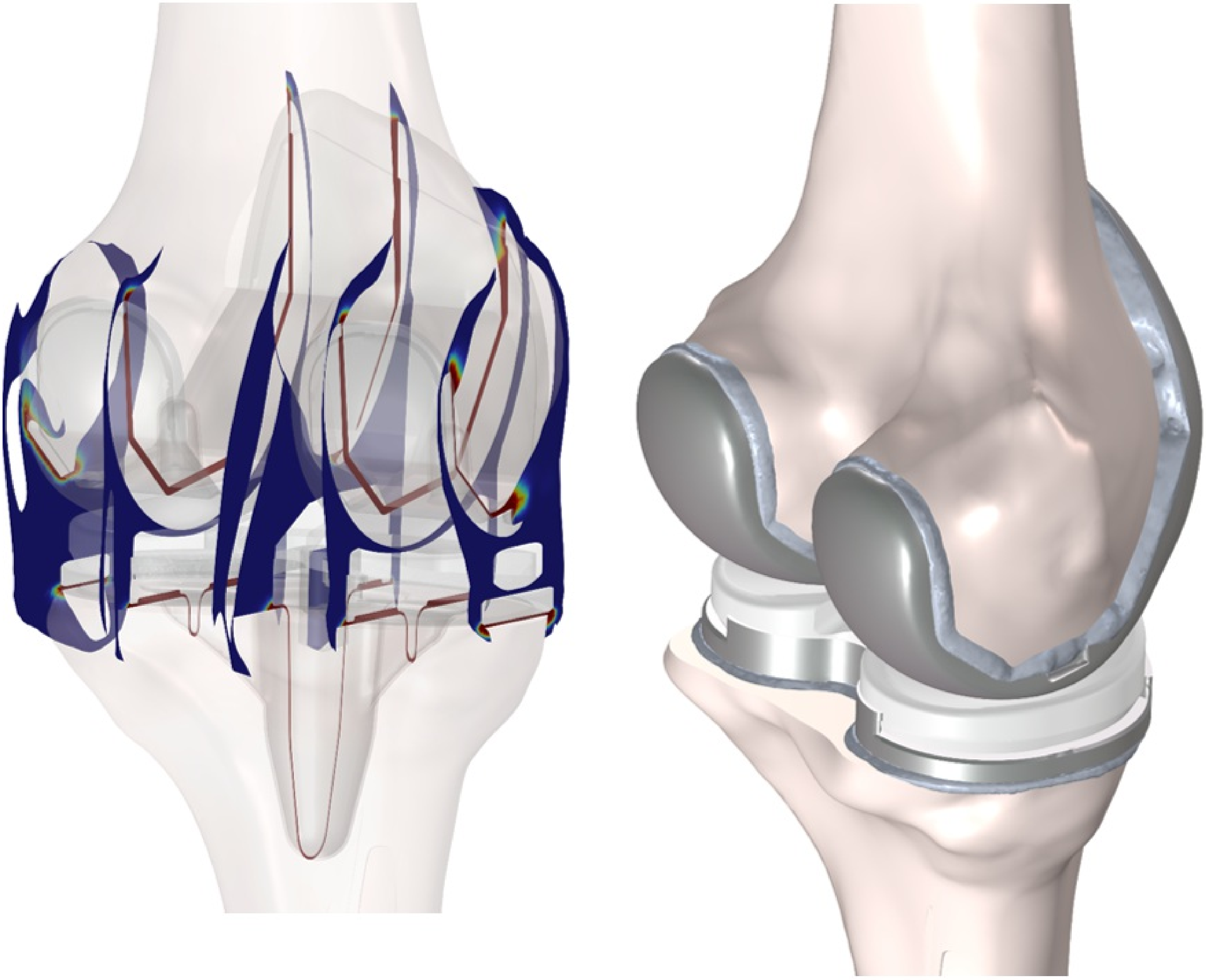

Figure 3 : Two views of cement region binding implant metal to bone

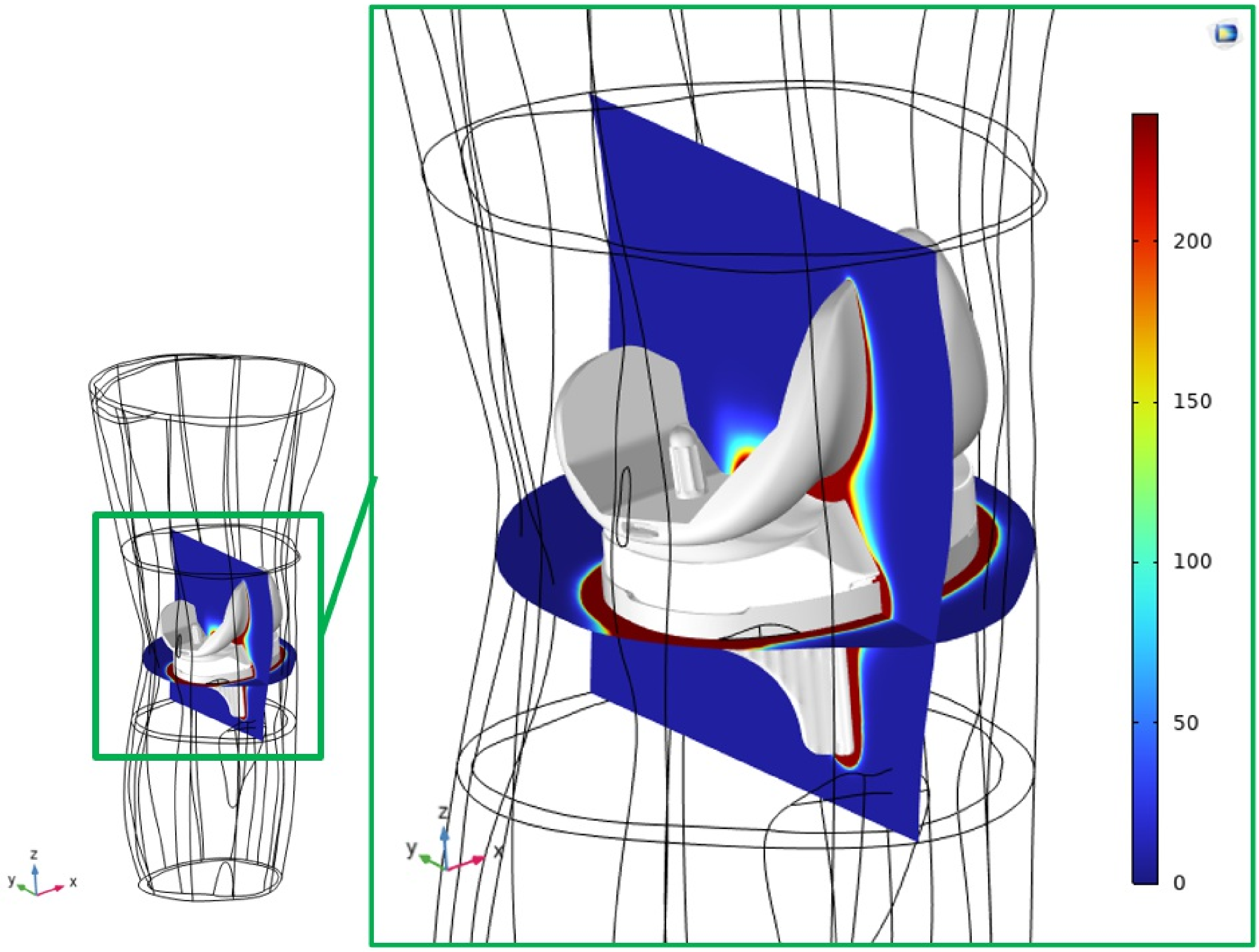

Figure 4 : CEM43 in tissue after heating treatment